Heliyon 10 (2024) e33238

Contents lists available at ScienceDirect

Heliyon

journal homepage: www.cell.com/heliyon

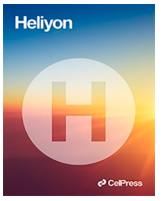

Research article

Development of an aptasensor for highly sensitive detection of cardiac troponin I using cobalt–nickel metal-organic framework (CoNi-MOF)

Ramya Devaraj *, Ashok Kumar Loganathan, Lalithambigai Krishnamoorthy

Department of Electrical & Electronics Engineering, PSG College of Technology, Coimbatore, India

ARTICLE INFO

Keywords:
Cardiac troponin
Aptamer
Metal-organic framework
Electrochemical
Diagnostic sensor

ABSTRACT

Objective and rationale: This study aimed to develop a highly sensitive and selective single-stranded DNA (ssDNA) aptamer targeting cardiac troponin I (cTnI), a crucial biomarker for acute myocardial infarction (AMI). The objective was to fabricate a novel aptamer electrochemical sensor using a composite material of cobalt-nickel metal-organic framework (CoNi-MOF) on screen-printed carbon electrodes (SPCE), leveraging the composite's large surface area and excellent electrical conductivity alongside the aptamer's high affinity for cTnI.

Methods: The aptamer electrochemical sensor was fabricated using the CoNi-MOF composite on SPCE and characterized its properties. They conducted electrochemical measurements to assess the sensor's performance in detecting cTnI. The sensor's stability, reproducibility, and electro-catalytic activity were evaluated.

Results: The sensor demonstrated linear detection of cTnI over a concentration range of 5–75 pg/mL, with a low limit of detection (LOD) of 13.2 pM. Remarkable stability and reproducibility were observed in cTnI detection. The sensor exhibited exceptional electro-catalytic activity, enabling accurate quantification of cTnI levels in various solutions.

Conclusions: This research presents a significant advancement towards the development of reliable, cost-effective, and easily deployable cTnI sensors for clinical applications. The sensor's versatility in detecting cTnI across different concentration ranges highlights its potential utility in diverse clinical settings, particularly for early detection and monitoring of cardiac conditions.

1. Introduction

Cardiovascular disease (CVD) remains the leading global cause of mortality, with acute myocardial infarction (AMI) contributing significantly [1]. Cardiac biomarkers, such as cardiac troponin I (cTnI), are released into the bloodstream in response to heart muscle damage or stress and play a critical role in diagnosing heart diseases, particularly AMI [2]. While various biomarkers exist, cTnI stands out for its specificity towards cardiomyocytes, the specialized muscle cells within the heart. Biosensors have emerged as powerful tools for detecting and quantifying biomolecules, including biomarkers, thereby leveraging advancements in biology and technology [3]. Electrochemical biosensors are particularly notable among biosensor technologies owing to their versatility and sensitivity. These biosensors typically comprise a bio-recognition element, electrode interface, and electrochemical transducer, making them ideal for

* Corresponding author.
E-mail address: ramyabmie@gmail.com (R. Devaraj).

https://doi.org/10.1016/j.heliyon.2024.e33238
Received 15 April 2024; Received in revised form 3 June 2024; Accepted 17 June 2024
Available online 19 June 2024

biomarker detection [4–7].

Conventional antibody-based sensors and carbon-based materials, particularly carbon nanotubes (CNT), and reduced graphene oxide (rGO) have shown promise in electrochemical detection [8–10]. However, they suffer from limitations such as sensitivity to environmental conditions, high production costs, limited availability, and stability issues [11–14]. To address these challenges, researchers are exploring alternative bio-recognition elements, such as aptamers [15]. Aptamers, short, single-stranded DNA or RNA molecules, offer advantages such as easy synthesis, increased stability, and greater specificity. Electrochemical aptasensors have emerged as promising tools for the sensitive and selective detection of biomarkers, including cardiac troponin I (cTnI), a crucial indicator of acute myocardial infarction (AMI) [16]. To further enhance sensor performance, researchers are incorporating metal-organic frameworks (MOFs) into aptasensor platforms, capitalizing on their unique properties. MOFs offer large surface areas, diverse functionalities, and tunable pore structures, all of which are essential for improving sensor performance. The high surface area and porosity of MOFs enable increased analyte capture, resulting in enhanced sensitivity. Moreover, the customizable structural properties of MOFs allow for precise tailoring to meet specific biosensing requirements through the modification of organic ligands. This adaptability ensures improved stability and conductivity, maintaining consistent sensor performance across diverse environments, including physiological conditions, environmental hazards, and wearable sensors [17–23].

Although monometallic MOFs such as Cu-MOFs and Cr-MOFs have been used in biosensing applications, they frequently encounter sensitivity and stability limitations. For instance, Hatami et al. (2019) developed a Cu-MOF-RGO nanocomposite-based aptasensor for MUC1 detection, achieving enhanced stability and reproducibility [24]. However, the inherent properties of monometallic MOFs can restrict their overall performance. In contrast, bimetallic MOFs, such as ZnZr and TbFe, offer significant advantages. Zhou et al. (2019) created a ZnZr bimetallic MOF aptasensor for detecting membrane protein tyrosine kinase-7 (PTK7), achieving a promising linear range [25]. Similarly, Wang et al. (2019) synthesized TbFe-MOF nanostructures for detecting CA125 and MCF-7 cells, demonstrating high sensitivity, excellent biocompatibility, and low detection limits [26]. These bimetallic frameworks offer superior performance characteristics, rendering them well-suited for advanced biosensing applications. Therefore, the primary focus of this research is to investigate an aptamer-based electrochemical biosensor, that incorporates Cobalt–Nickel MOF to enhance conductivity and enable accurate and sensitive detection of cTnI, facilitating early diagnosis of AMI in human plasma. In addition to the integration of Cobalt–Nickel MOF, the study also optimizes key parameters, such as the concentration of aptamers and the incubation time, to enhance the sensitivity of the aptasensor developed in this study. By systematically fine-tuning these parameters, the aptasensor achieves superior performance in detecting cTnI, enabling early diagnosis of acute myocardial infarction (AMI) with high sensitivity and accuracy.

2. Materials and methods

2.1. Materials

Cardiac Troponin I from the human heart (cTnI), Bovine Serum Albumin (BSA), (3-dimethylaminopropyl)-3-ethylcarbodiimide hydrochloride (EDC), and N-hydroxy succinimide (NHS) were acquired from Sigma Aldrich (USA). The amine-terminated complementary aptamer sequence for cTnI (5′–NH_2–$(CH_2)_6$-CGTGCAGTACGCCAACCTTTCTCATGCGCTGCCCCTCTTA-3′) was synthesized from Priority Lifescience in Coimbatore. Spectrum supplied cobalt (II) nitrate hexahydrate (Co $(NO_3)_2 6H_2O$), whereas aluminium nitrate hexahydrate (Al $(NO_3)_3 9H_2O$) and nickel nitrate hexahydrate (Ni $(NO_3)_2 6H_2O$) were used as metal precursors. The linkers used were 4, 4′-bipyridine and 1, 3, 5-benzene tricarboxylic acid, both from Ottokemi and SRL chemicals. Pure Chems supplied the solvent of choice, N, N-dimethylformamide (DMF). All the compounds utilized in this investigation were of analytical quality and did not require additional purification.

2.2. Instrumentation for characterization and electrochemical

Field Emission Spectroscopy was used to analyze the morphological of the synthesized material (Carl Zeiss Microscopy). A Fourier transform infrared spectrometer (Shimadzu IR affinity, Japan) with a spectrum range of 400–2000 cm^{-1} was used to analyze the functional group properties of the newly synthesized compound CoNi-MOF. Energy dispersive X-ray spectroscopy (Bruker Quantex EDS X-ray Spectrophotometer) was used to evaluate the morphological changes in these MOF. A monochromatic Cu Ka radiation ($\lambda =$ 1.54 Å) was used with an X-ray diffractometer (XRD, Empyrean, Malvern Panalytical, United Kingdom) to examine the phase structure and crystal arrangement of the materials. An Admiral Squidstat Plus electrochemical workstation was also used for electrochemical experiments, notably differential pulse voltammetry (DPV), electrochemical impedance spectroscopy (EIS) and cyclic voltammetry (CV).

2.3. Synthesis of bimetallic MOFs

The experiment began by introducing 1.38g of cobalt (II) nitrate hexahydrate, 1.38g of nickel nitrate hexahydrate, 0.004g of benzene tricarboxylic acid, and 0.74 g of 4,4′-bipyridine into a beaker holding 1.32 ml of Triethylamine, and 80 ml of N, N-dimethylformamide (DMF). This mixture was later transferred into a Teflon autoclave reactor and maintained at a temperature of 120 °C for 24 h. Afterward, the solution was allowed to cool down to room temperature. The resulting product was subjected to a thorough washing and filtration process involving ethanol, DMF, and water. The filtered material, known as CoNi-MOF, was then dried at 60 °C for 24 h [27].

2.4. Preparation of bimetallic MOF/SPCE electrode

The preparation of the Bimetallic MOF-modified Screen-Printed Carbon Electrode (SPCE) involved a meticulous step-by-step electrochemical deposition process shown in Scheme 1. The MOF was deposited onto the SPCE in a 1:1 ratio of K_3 [Fe (CN) $_6$] and the synthesized MOF, with 30 ml of phosphate-buffered saline (PBS) used. This electrodeposition process was conducted for sixty cycles, employing a scan rate of 100 mV per second within the potential range of −0.6 V–0.8 V. Subsequently, the freshly prepared Bimetallic MOF-modified SPCE underwent a thorough cleaning with water and was left to air dry at room temperature.

2.5. Fabrication of cTnI aptamer complex-enhanced bimetallic (Co, Ni) MOF on SPCE (cTnI/aptamer/CoNi-MOF/SPCE)

The reactivity of the prepared bimetallic CoNi-MOF coated SPCE was enhanced by uniformly activating the –COOH groups across the electrode surface. This promotes efficient binding stability and increases sensor specificity. Surface functionalization was achieved by drop-casting a mixture of 1-ethyl-3-(3-dimethylaminopropyl) carbodiimide (EDC) and N-hydroxy succinimide (NHS) chemistry, followed by a 20-min incubation [28]. After functionalization, an amine-modified aptamer was prepared in a binding buffer holding potassium chloride, sodium chloride, magnesium chloride and phosphate buffer solution. This aptamer specific to the cardiac troponin I biomarker was hybridized onto the activated MOF/SPCE surface and dried using nitrogen gas forming amide bonds with amino groups present on the aptamer. The aptamer provides selective detection and specificity towards cTnI in complex biological samples. A 4 μM solution (10 μL) of the cardiac troponin I aptamer was drop cast onto the prepared bimetallic CoNi-MOF coated SPCE for precise coverage on the electrode over 21 h. The bio-functionalized Apt-cTnI/NOF/SPCE electrodes were stored in a refrigerator at 4 °C for future use. Subsequently, a solution of the biomarker cTnI was drop cast onto the aptamer/CoNi-MOF/SPCE at room temperature for 40 min to form the aptamer-cTnI complex. The modified electrode was then rinsed with distilled water to remove any unbound cTnI-aptamer [29].

2.6. Electrochemical detection of cTnI using fabricated aptasensor

The electrochemical behavior of the modified nanosensors is evaluated using cyclic voltammetry (CV) and differential pulse voltammetry (DPV) at various stages which includes material deposition, biofunctionalization of the electrode with aptamer and bioconjugation with cTnI biomarker. A solution holding potassium ferricyanide was used as an electrolyte for all electrochemical studies. The scan rate for CV was 100 mV/s with the potential range of −0.6 V – +0.8 V. Cyclic Voltammetry (CV) and differential pulse voltammetry (DPV) after aptamer binding on MOF/SPCE provided the electrochemical properties of the modified sensor by studying the peak current changes. Similarly, CV and DPV studies after cTnI binding to aptamers were conducted. The change in peak current shows the presence and concentration of cTnI.

3. Results and discussions

3.1. Characterization of bimetallic MOF and bimetallic MOF/SPCE electrode

3.1.1. Basic characterization of bimetallic MOF

The materials prepared initially underwent powdered X-ray diffraction (PXRD) analysis to verify their crystalline nature and the formation of MOF-derived materials. The PXRD results, as depicted in Fig. 1, show characteristic peaks corresponding to CoNi-MOF. The observed high-intensity peaks closely align with previously reported data, confirming the consistency in the material's crystalline structure. Specifically, the obtained high-intensity diffraction peaks for CoNi at 2θ values of 12.3, 12.9, 14.51, 15.59, 16.27, 17.131, 18.66, 21.89, 23.94, and 26.11° precisely match the pattern from earlier studies [30,31] (see Fig. 1).

Using Raman spectroscopy, the distinctive peaks associated with the metal-organic linker bonding in Co–Ni–BTC were further examined. At 1006 cm^{-1}, the benzene ring with ν (C═C) displays stretching vibration. The stretching vibration of ν (COO^-), which is symmetric and asymmetric, is primarily responsible for the peaks at 1464 and 1525 cm^{-1}. As a result of the effective synthesis of Co-BTC MOF, Fig. 2 displays strong peaks at 471 and 667 cm^{-1}, which correspond to the ν Co–O) stretching vibration. At 423 cm^{-1}, the important ν(Ni–O) stretching vibration was detected. The separate monometallic MOFs (Co-MOFs and Ni-MOFs) are compared and matched with the bimetallic CoNi-MOF [32].

The CoNi-MOFs FT-IR spectrum displays distinctive characteristics indicating metal coordination with the BTC linker. The

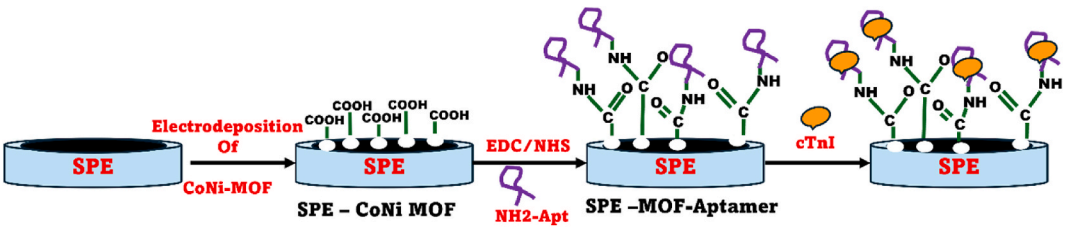

Scheme 1. Schematic representation of aptamer based electrochemical detection of Cardiac Troponin-I.

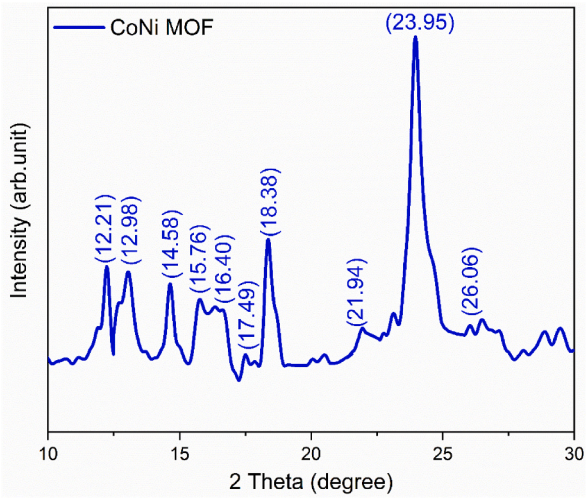

Fig. 1. XRD pattern for CoNi-MOF.

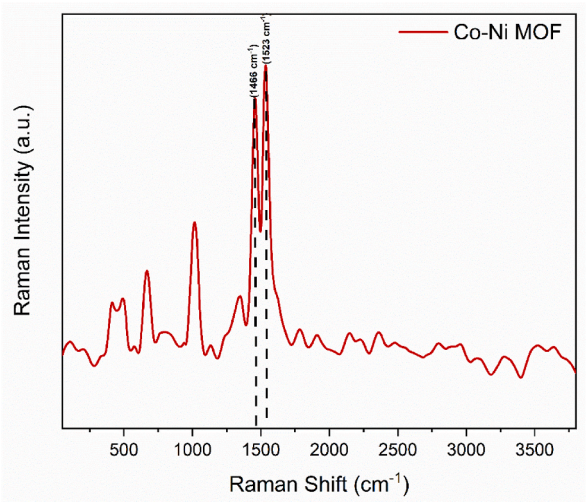

Fig. 2. Raman spectra of CoNi-MOF.

symmetric and asymmetric stretching modes of the coordinated (–COO–) group are evident in the strong absorption bands observed at 1620, 1575, 1441, and 1380 cm^{-1}, respectively. The absence of absorption bands between 1730 and 1690 cm^{-1} suggests the deprotonation of H_3BTCs upon contact with metal ions. There is no absorption by the –COOH groups, supporting the transition of H_3BTC. In the CoNi BTC spectrum, a significant new band emerges between 758 and 722 cm^{-1} attributed to the out-of-plane vibration of the organic ligands within the 1, 3, 5-substituted benzene core. Additionally, the stretching vibrations ring δ-OH and para-aromatic CH groups are associated with the band at 639 cm^{-1}. These findings shed light on the complex dynamics of the CoNi-MOF system, revealing structural changes resulting from the interaction between the metal ions and the organic ligands [33,34] (see Fig. 3).

An energy-dispersive X-ray spectrometer and a FE-SEM were used to assess the morphological changes of the MOFs. Fig. 4(a and b) illustrates the surface morphology of the CoNi-MOFs showing a nanolayered sheet morphology indicative of a more robust and compact topology. EDX elemental mapping (Fig. 4(c–h) revealed well-distributed elements (C, N, O, Co, and Ni) within the synthesized MOF. Additionally, the EDAX images demonstrate the presence of metal ions in the synthesized MOF (Figure S1). Table S1 displays the percentage of elemental weight in the materials that were synthesized.

3.2. Aptasensor electrochemical performance for cTnI detection

The electrochemical performance of the SPCE was assessed during the aptamer immobilization on the CoNi-modified surface electrode using a 5.0 mM $[Fe(CN)_6]^{3-/4-}$ solution holding 0.1 M KCl (Fig. 5). In Fig. 5, a series of cyclic voltammetry (CV) scans show the redox response of the modified SPCE. Compared to the bare SPCE, there is a significant increase in the redox peak due to the

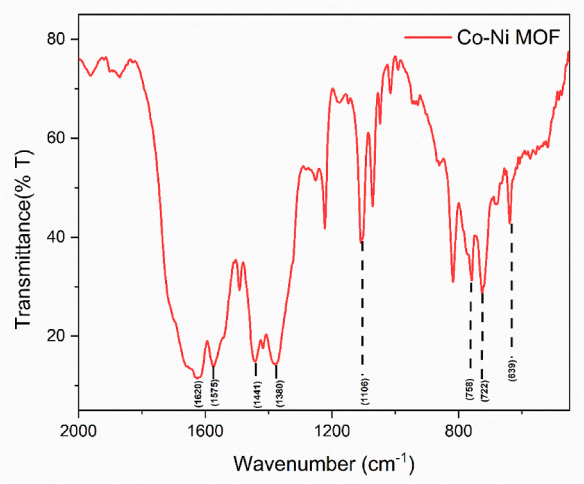

Fig. 3. FT-IR Spectra profile of CoNi-MOF.

excellent conductivity and electron transfer of the CoNi-MOF. The immobilization of the aptamer cTnI was then conducted, resulting in a further decrease in the peak current due to the decrease in conductivity, confirming the bonding of the aptamer to the modified electrode surface. Similarly, Electrochemical impedance spectroscopy (EIS) measurements were conducted using a 5 mV AC voltage, 200 mV applied potential, and frequency range of 10 mHz–100 kHz (Fig. 6). The bare SPE had a small semicircle diameter, which further decreased with CoNi-MOF, indicating enhanced electron transfer. Upon aptamer assembly on CoNi-MOF/SPE, the semicircle diameter increased, implying that the aptamer hindered electron transfer due to its poor conductivity. This suggests that CoNi-MOF improves conductivity, while the aptamer reduces it by obstructing electron flow.

The charge transfer efficiency at the electrode interface for cTnI detection is significantly influenced by the concentration of AcTnI. The DPV signal of the CoNi-MOF/SPCE is affected by varying concentrations of AcTnI, as seen by the graph in Fig. 7(a). Interestingly, the DPV response significantly decreases at concentrations of 4 μM, indicating possible saturation of the sensor's surface active. Surface crowding resulting from this saturation may hinder the aptamers' efficient binding to cTnI. Consequently, the optimal concentration for the aptamer sensor was 4 μM AcTnI. Additionally, the incubation period of cTnI significantly influences its detection. The electrochemical signal remains largely unaffected when cTnI is incubated for more than 40 min, as shown in Fig. 7(b). This suggests a saturation of the bioaffinity between the cTnI target and AcTnI on the electrode surface. Conversely, the spatial potential resistance effect causes the current response to stabilize, reducing sensitivity to the target. Thus, we determined that a 40-min incubation period was ideal.

The differential pulse voltammetry results show a noticeable decrease in the peak of the AcTnI/CoNi-MOF/SPCE electrode in response to varying cardiac troponin I concentrations. Fig. 8(a) presents the electrochemical signal of DPV in a 5.0 mM $[Fe(CN)_6]^{3-/4-}$ solution with 0.1 M KCl, while Fig. 8(b) illustrates the relationship between the reduction peak current and the concentration of cTnI. It demonstrates a linear correlation with the peak value for the various cTnI concentration ranges examined, which were 5 pg/ml to 75 pg/ml. The aptasensor built has a low detection limit of 13 pM and a sensitivity of 15.22 μA/pg/ml indicating its capability to detect cTnI at extremely low concentrations. Therefore, this aptasensor exhibits sufficient sensitivity for cTnI detection.

Table 1 compares the analytical performance of various electrochemical biosensors using different materials for detecting the cTnI biomarker. The aptamer-based CoNi-MOF electrochemical sensor exhibited a satisfactory linear range with a superior limit of detection. The stability of the aptamer sensor was further assessed by measuring the DPV current of the modified electrode after one month. The electrochemical signal before and after storage showed a slight change, with a 6.2 % decrease in the peak DPV (Fig. S2). This indicates the excellent stability of the proposed electrochemical aptamer sensor for cTnI detection. Additionally, the specificity of the modified sensor was evaluated by storing the AcTnI/CoNi-MOF/SPCE at 4 °C for 30 days (Fig. 9). The proposed aptamer sensor demonstrates excellent selectivity and a remarkable ability to resist interference.

4. Conclusions

In this study, we developed highly sensitive and selective ssDNA aptamers against cTnI, a diagnostic biomarker of AMI. An aptamer electrochemical sensor was constructed using CoNi-MOF/SPCE, combining the large surface area and good electrical conductivity of the composite with the high affinity and specificity of the aptamer. The sensor could linearly detect cTnI at concentrations of 5, 10, 15, 25, 50, and 75 pg/ml with a low LOD of 13.2 pM. The sensor showed excellent stability and reproducibility in the detection of cTnI, making it a promising candidate for clinical applications. The success of our electrode in accurately quantifying cTnI levels in diverse solutions was attributed to the exceptional electrocatalytic activity of the aptasensor. This research opens new avenues for the development of reliable, cost-effective, and readily deployable cardiac troponin I, with broad implications for healthcare and diagnostics. The ability of this sensor to detect cTnI across a wide range of concentrations highlights its potential for use in various

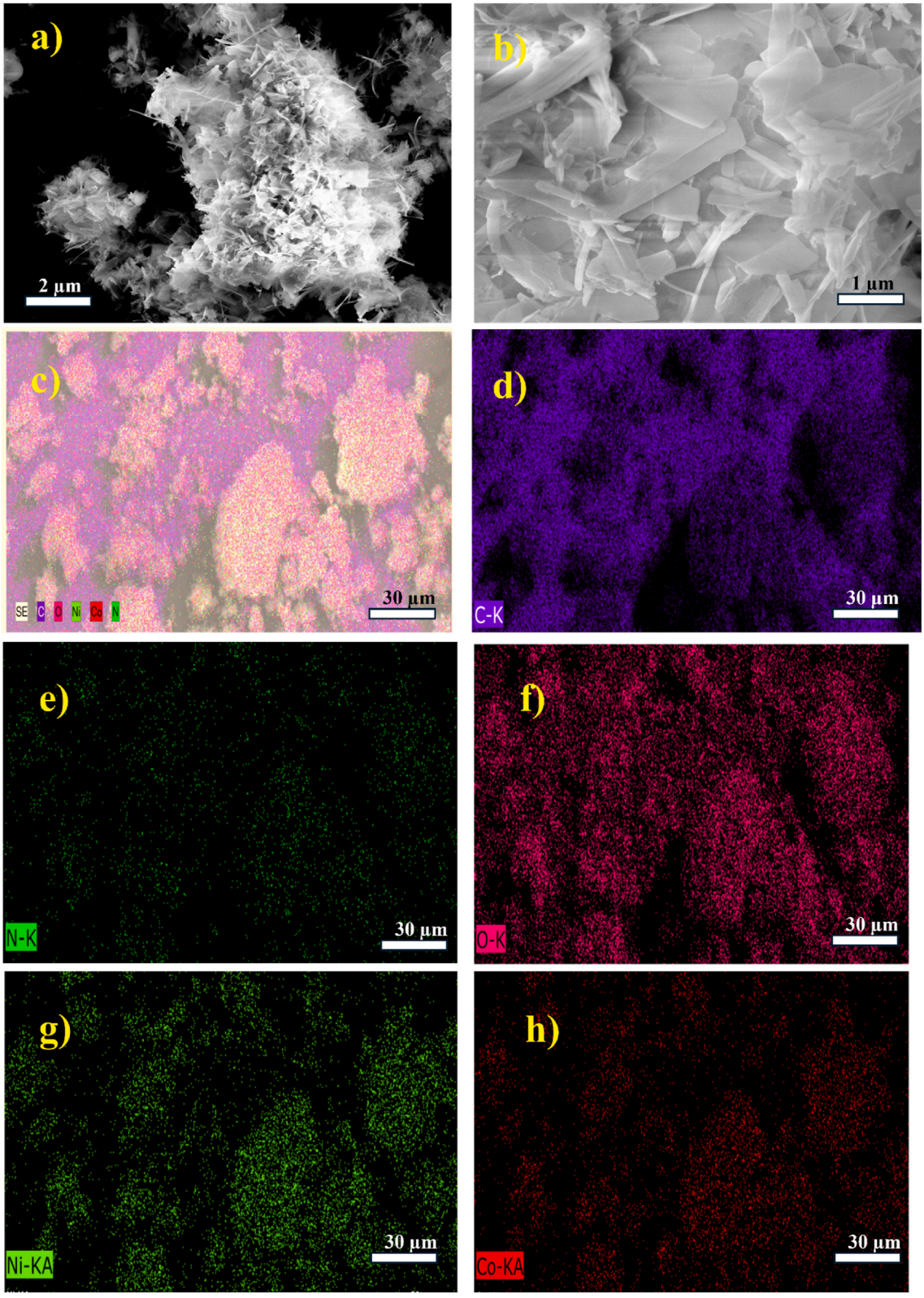

Fig. 4. (a–b) FE-SEM image of CoNi-MOF, (c–h) colour mapping results of CoNi-MOF, (c) mixed colour mapping, (d–h) mapping results of C, N, O, Ni and Co respectively.

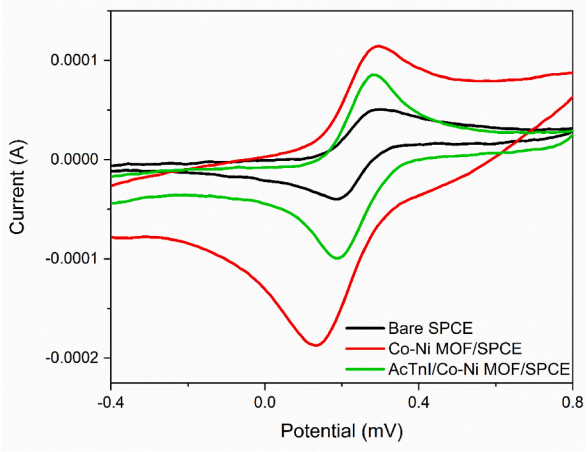

Fig. 5. CV of Bare SPCE, CoNi-MOF/SPCE and AcTnI/CoNi-MOF/SPCE in 50 mV/s Scan rate.

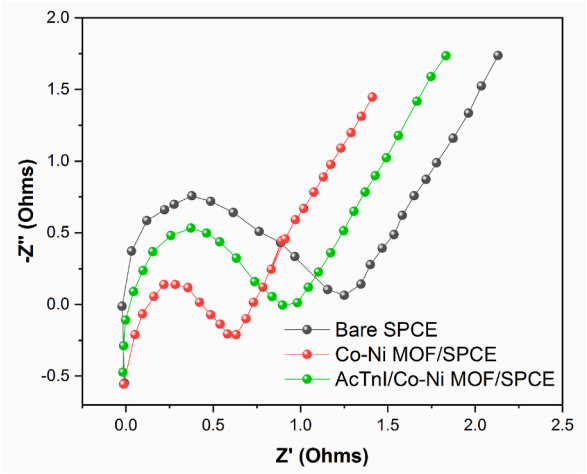

Fig. 6. EIS characterisation of bare SPCE(black), CoNi-MOF/SPCE(red), AcTnI/CoNi-MOF/SPCE(green).

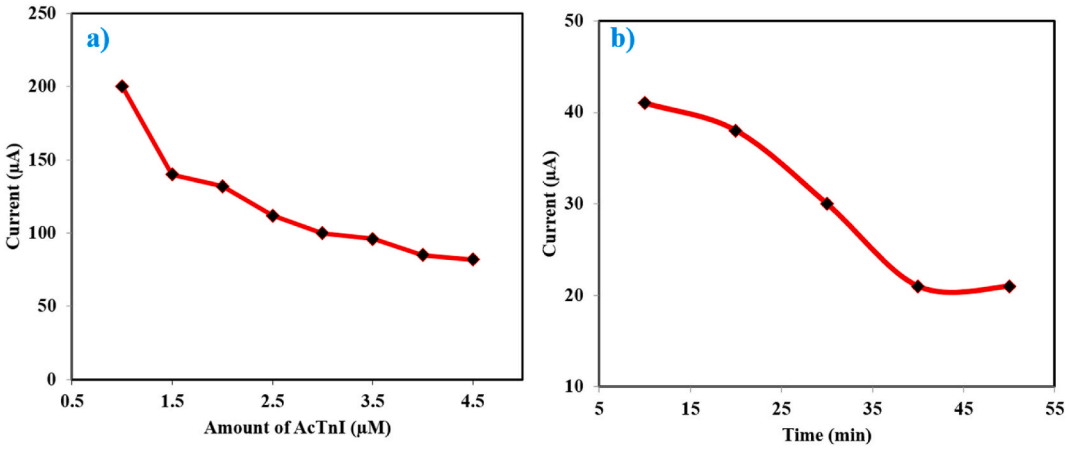

Fig. 7. The role of (a) AcTnI concentration and (b) incubation duration on sensing efficiency.

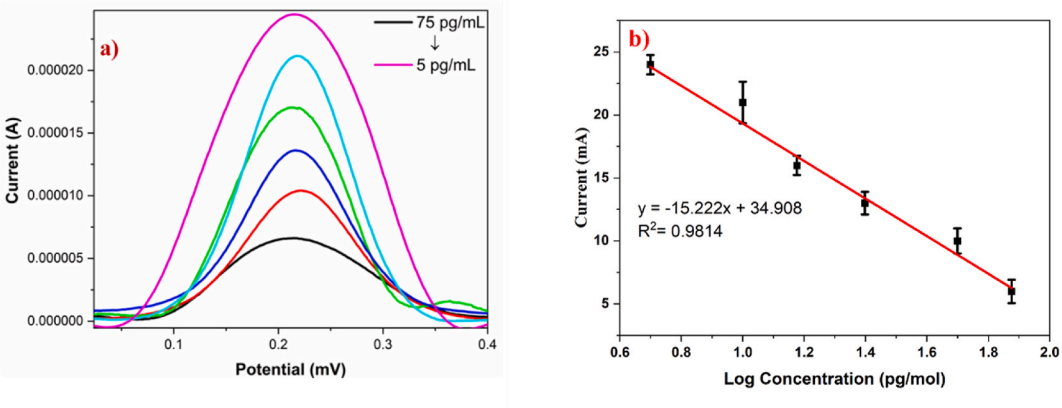

Fig. 8. a) DPV curves of AcTnI/CoNi-MOF/SPCE in relation to 5 pg/ml, 10 pg/ml, 15 pg/ml, 25 pg/ml, 50 pg/ml, and 75 pg/ml (b) Linear correlation between current and logarithm of cTnI concentrations.

Table 1
Performance comparison of different electrochemical biosensors.

Materials	Method	LOD	Linear range	Reference
CNF	EIS	0.2 ng/mL	0.25–1 ng/mL	[35]
Nanostructured ZrO_2	CV	0.1 ng/mL	0.1–100 ng/mL	[36]
DIL – Helical CNT	DPV	0.02 ng/mL	0.05–30 ng/mL	[37]
GC/N-proGO-aptamer	DPV	0.94 pg/ml	0.001–100 ng/ml	[38]
CoNi-MOF – Aptamer based	DPV	13.2 pM (0.31 pg/mL)	5–75 pg/mL	This work

CNF: carbon nanofiber; ZrO_2: Zirconium oxide; DIL: dialdehyde-functionalized ionic liquid; CNT: carbon nanotube; GC: glassy carbon electrode; N-proGO: nitrogen-doped reduced graphene oxide; CoNi-MOF: Cobalt Nickel metal organic framework; EIS: electrochemical impedance spectroscopy; CV: cyclic voltammetry: DPV: Differential Pulse voltammetry.

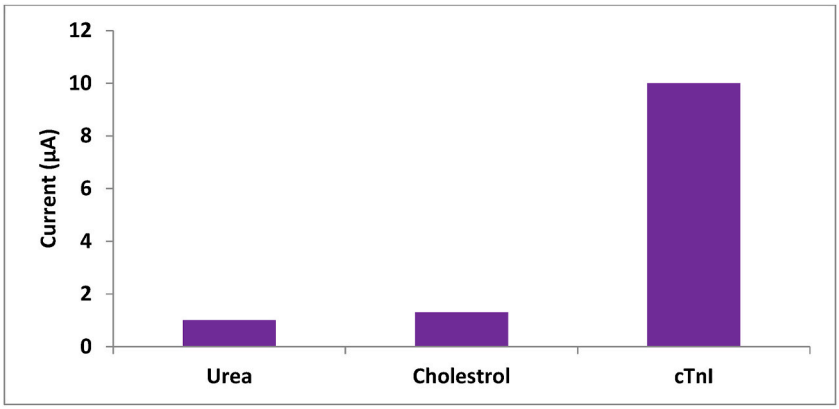

Fig. 9. Selectivity evaluation of the sensor.

clinical settings. Additionally, the sensitivity and specificity of the electrode make it a valuable tool for the early detection and monitoring of cardiac conditions. Further studies are needed to validate the performance of the aptasensor in complex biological matrices such as blood serum. Once these validations are completed, the aptasensor can revolutionize the field of cardiac biomarker detection and monitoring.

Funding

The research was financially funded by the Department of Health Research, Ministry of Health and Family Welfare, under the Indian Council of Medical Research (ICMR) ID. No.2021-9388 (File No. 17× (3)/Adhoc/7/2022-ITR).

Data availability statement

Data will be made available on request.

CRediT authorship contribution statement

Ramya Devaraj: Writing – review & editing, Writing – original draft, Methodology, Investigation, Formal analysis, Data curation, Conceptualization. **Ashok Kumar Loganathan:** Writing – review & editing, Writing – original draft, Supervision, Project administration, Investigation, Funding acquisition. **Lalithambigai Krishnamoorthy:** Writing – review & editing, Writing – original draft, Methodology, Data curation.

Declaration of competing interest

The authors declare the following financial interests/personal relationships which may be considered as potential competing interests: AshokKumar Loganathan reports financial support was provided by Indian Council of Medical Research. If there are other authors, they declare that they have no known competing financial interests or personal relationships that could have appeared to influence the work reported in this paper.

Acknowledgements

The authors would like to thank the Electrical and Electronics Engineering Department of PSG College of Technology, Coimbatore for the support. The research was financially funded by the Department of Health Research, Ministry of Health and Family Welfare, under the Indian Council of Medical Research (ICMR) ID. No.2021-9388 (File No. 17×(3)/Adhoc/7/2022-ITR).

Appendix A. Supplementary data

Supplementary data to this article can be found online at https://doi.org/10.1016/j.heliyon.2024.e33238.

References

[1] M.D. Cesare, H. Bixby, T. Gaziano, L. Hadeed, C. Kabudula, D.V. McGhie, J. Mwangi, B. Pervan, P. Perel, D. Piñeiro, S. Taylor, F. Pinto, World Heart Report 2023: Confronting the World's Number One Killer, 2023, pp. 1–52.
[2] S.H. Tveit, P.L. Myhre, T.A. Hanssen, S.H. Forsdahl, A. Iqbal, T. Omland, H. Schirmer, Cardiac troponin I and T for ruling out coronary artery disease in suspected chronic coronary syndrome, Sci. Rep. 12 (2022) 1–9, https://doi.org/10.1038/s41598-022-04850-7.
[3] B. Senf, W.H. Yeo, J.H. Kim, Recent advances in portable biosensors for biomarker detection in body fluids, Biosensors 10 (2020), https://doi.org/10.3390/BIOS10090127.
[4] M. Pohanka, P. Skládal, Electrochemical biosensors - principles and applications, J. Appl. Biomed. 6 (2008) 57–64, https://doi.org/10.32725/jab.2008.008.
[5] M.S. Sumitha, T.S. Xavier, Recent advances in electrochemical biosensors – a brief review, Hybrid Adv 2 (2023) 100023, https://doi.org/10.1016/j.hybadv.2023.100023.
[6] N. Sandhyarani, Surface Modification Methods for Electrochemical Biosensors, Elsevier Inc., 2019, https://doi.org/10.1016/B978-0-12-816491-4.00003-6.
[7] Y. Ding M, S. Ding, D. Du, X. Wang, X. Hu, P. Guan, Z. Lyu, Recent Lin, Advances in electrochemical biosensors for the detection of Aβ42, a biomarker for Alzheimer disease diagnosis, TrAC, Trends Anal. Chem. (2023) 117087, https://doi.org/10.1016/j.trac.2023.117087.
[8] H. Meskher H, F. Achi, A. Zouaoui, S. Ha, M. Peacock, Belkhalfa, Simultaneous and selective electrochemical determination of catechol and hydroquinone on a nickel oxide (NiO) reduced graphene oxide (rGO) doped multiwalled carbon nanotube (fMWCNT) modified platinum electrode, Anal. Lett. 55 (2022) 1466–1481, https://doi.org/10.1080/00032719.2021.2008951.
[9] F. Meskher, H, Achi, Electrochemical sensing systems for the analysis of catechol and hydroquinone in the aquatic environments: a critical review, Crit. Rev. Anal. Chem. (2022) 1–14, https://doi.org/10.1080/10408347.2022.2114784.
[10] R. MeskherH., Thakur, A.K., Sharifianjazi, F., Sathyamurthy, R., Lynch, I. and Saidur, MXene-CNTs: A Prospective Composite Material for Biomedical Applications Engrossing Wearable Sensors, Age of MXe, ACS Publications, n.d. https://doi.org/10.1021/bk-2023-1443.ch004.
[11] W. Xu, D. Wang, D. Li, C.C. Liu, Recent developments of electrochemical and optical biosensors for antibody detection, Int. J. Mol. Sci. 21 (2020), https://doi.org/10.3390/ijms21010134.
[12] Y. Ning, J. Hu, F. Lu, Aptamers used for biosensors and targeted therapy, Biomed. Pharmacother. 132 (2020) 110902.
[13] H. Meskher, T. Ragdi, A.K. Thakur, S. Ha, I. Khelfaoui, R. Sathyamurthy, S.W. Sharshir, A.K. Pandey, R. Saidur, P. Singh, F. Sharifianjazi, I. Lynch, A review on CNTs-based electrochemical sensors and biosensors: unique properties and potential applications, Crit. Rev. Anal. Chem. 1 (2023) 1–24, https://doi.org/10.1080/10408347.2023.2171277.
[14] H. Meskher, H.C. Mustansar, A.K. Thakur, R. Sathyamurthy, I. Lynch, P. Singh, T.K. Han, R. Saidur, Recent trends in carbon nanotube (CNT)-based biosensors for the fast and sensitive detection of human viruses: a critical review, Nanoscale Adv. 5 (2022) 992–1010, https://doi.org/10.1039/d2na00236a.
[15] X. Zhao, S. Li, G. Liu, Z. Wang, Z. Yang, Q. Zhang, M. Liang, J. Liu, Z. Li, Y. Tong, G. Zhu, X. Wang, L. Jiang, W. Wang, G.Y. Tan, L. Zhang, A versatile biosensing platform coupling CRISPR–Cas12a and aptamers for detection of diverse analytes, Sci. Bull. 66 (2021) 69–77, https://doi.org/10.1016/j.scib.2020.09.004.
[16] M. Mahmoudpour, S. Ding, Z. Lyu, G. Ebrahimi, D. Du, J. Ezzati Nazhad Dolatabadi, M. Torbati, Y. Lin, Aptamer functionalized nanomaterials for biomedical applications: recent advances and new horizons, Nano Today 39 (2021) 101177, https://doi.org/10.1016/j.nantod.2021.101177.
[17] K. Nemčeková, J. Labuda, Advanced materials-integrated electrochemical sensors as promising medical diagnostics tools: a review, Mater. Sci. Eng. C 120 (2021), https://doi.org/10.1016/j.msec.2020.111751.
[18] H.S. Wang, Metal–organic frameworks for biosensing and bioimaging applications, Coord. Chem. Rev. 349 (2017) 139–155, https://doi.org/10.1016/j.ccr.2017.08.015.
[19] A. Gupta, S.K. Sharma, V. Pachauri, S. Ingebrandt, S. Singh, A.L. Sharma, A. Deep, Sensitive impedimetric detection of troponin I with metal-organic framework composite electrode, RSC Adv. 11 (2021) 2167–2174, https://doi.org/10.1039/d0ra06665f.

[20] X. WeiX, W. Song, Y. Fan, Y. Sun, Z. Li, S. Chen, J. Shi, D. Zhang, X. Zou, A. Xu, SERS aptasensor based on a flexible substrate for interference-free detection of carbendazim in apple, Food Chem. 431 (2024) 137120.
[21] H. Meskher, S.B. Belhaouari, F. Sharifianjazi, Mini review about metal organic framework (MOF)-based wearable sensors: challenges and prospects, Heliyon 9 (2023) e21621, https://doi.org/10.1016/j.heliyon.2023.e21621.
[22] H. Meskher, F. Achi, S. Ha, B. Berregui, F. Babanini, H. Belkhalfa, Sensitive rGO/MOF based electrochemical sensor for penta-chlorophenol detection: a novel artificial neural network (ANN) application, Sensors and Diagnostics 1 (2022) 1032–1043, https://doi.org/10.1039/d2sd00100d.
[23] M. Negahdary, L. Angnes, Recent advances in electrochemical nanomaterial-based aptasensors for the detection of cancer biomarkers. https://doi.org/10.1016/j.talanta.2023.124548, 2023.
[24] M. Hatami, Z. Jalali, F. Tabrizi, M.A. and Shamsipur, Application of metal-organic framework as redox probe in an electrochemical aptasensor for sensitive detection of MUC1, Biosens. Bioelectron. 141 (2019) 111433.
[25] S. Zhou N, F. Su, C. Guo, L. He, Z. Jia, M. Wang, Q. Jia, Z. Zhang, Lu, Two-dimensional oriented growth of Zn-MOF-on-Zr-MOF architecture: a highly sensitive and selective platform for detecting cancer markers, Biosens. Bioelectron. 123 (2019) 51–58.
[26] M. WangM, M. Hu, Z. Li, L. He, Y. Song, Q. Jia, Z. Zhang, Du, Construction of Tb-MOF-on-Fe-MOF conjugate as a novel platform for ultrasensitive detection of carbohydrate antigen 125 and living cancer cells, Biosens, Bioelectron. 142 (2019) 111536.
[27] M. Manivannan, V. Rajagopal, L. Krishnamoorthy, S. Dhanasurya, V. Suryanarayanan, M. Kathiresan, T. Raju, L.A. Jones, One pot synthesis and characterization of binary and ternary metal organic frameworks (MOFs) as tri-modal catalysts for thiophene electrooxidation, water splitting and 4-nitrophenol reduction, New J. Chem. 47 (2023) 6330–6341, https://doi.org/10.1039/d3nj00347g.
[28] H. Hashemzadeh, Z. Khadivi-Khanghah, A. Allahverdi, M.M. Hadipour, E. Saievar-Iranizad, H. Naderi-Manesh, A novel label-free graphene oxide nano-wall surface decorated with gold nano-flower biosensor for electrochemical detection of brucellosis antibodies in human serum, Talanta Open 7 (2023) 100215, https://doi.org/10.1016/j.talo.2023.100215.
[29] J. Li, S. Zhang, L. Zhang, Y. Zhang, H. Zhang, C. Zhang, X. Xuan, M. Wang, J. Zhang, Y. Yuan, A novel graphene-based nanomaterial modified electrochemical sensor for the detection of cardiac troponin I, Front. Chem. 9 (2021) 1–8, https://doi.org/10.3389/fchem.2021.680593.
[30] J. Hong, S.J. Park, S. Kim, Synthesis and electrochemical characterization of nanostructured Ni-Co-MOF/graphene oxide composites as capacitor electrodes, Electrochim. Acta 311 (2019) 62–71, https://doi.org/10.1016/j.electacta.2019.04.121.
[31] B. Ambrose, R. Madhu, A. Kannan, S. Senthilvel, M. Kathiresan, S. Kundu, Impact of ligand in bimetallic Co, Ni-Metal-Organic framework towards oxygen evolution reaction, Electrochim. Acta 439 (2023) 141714, https://doi.org/10.1016/j.electacta.2022.141714.
[32] S. Naik Shreyanka, J. Theerthagiri, S.J. Lee, Y. Yu, M.Y. Choi, Multiscale design of 3D metal–organic frameworks (M−BTC, M: Cu, Co, Ni) via PLAL enabling bifunctional electrocatalysts for robust overall water splitting, Chem. Eng. J. 446 (2022), https://doi.org/10.1016/j.cej.2022.137045.
[33] M.G. Radhika, B. Gopalakrishna, K. Chaitra, L.K.G. Bhatta, K. Venkatesh, M.K. Sudha Kamath, N. Kathyayini, Electrochemical studies on Ni, Co & Ni/Co-MOFs for high-performance hybrid supercapacitors, Mater. Res. Express 7 (2020) 54003, https://doi.org/10.1088/2053-1591/ab8d5d.
[34] W. Zheng, W. Bi, X. Gao, Z. Zhang, W. Yuan, L. Li, A nickel and cobalt bimetal organic framework with high capacity as an anode material for lithium-ion batteries, Sustain. Energy Fuels 4 (2020) 5757–5764, https://doi.org/10.1039/d0se00983k.
[35] A. Periyakaruppan, R.P. Gandhiraman, M. Meyyappan, J.E. Koehne, Label-free detection of cardiac troponin-I using carbon nanofiber based nanoelectrode arrays, Anal. Chem. 85 (2013) 3858–3863, https://doi.org/10.1021/ac302801z.
[36] S. Kumar, S. Kumar, S. Augustine, B.D. Malhotra, Protein functionalized nanostructured zirconia based electrochemical immunosensor for cardiac troponin i detection, J. Mater. Res. 32 (2017) 2966–2972, https://doi.org/10.1557/jmr.2017.102.
[37] Q. Shen, M. Liu, Y. Lü, D. Zhang, Z. Cheng, Y. Liu, H. Gao, Z. Jin, Label-Free electrochemical immunosensor based on a functionalized ionic liquid and helical carbon nanotubes for the determination of cardiac troponin i, ACS Omega 4 (2019) 11888–11892, https://doi.org/10.1021/acsomega.9b01152.
[38] F. Chekin, A. Vasilescu, R. Jijie, S.K. Singh, S. Kurungot, M. Iancu, G. Badea, R. Boukherroub, S. Szunerits, Sensitive electrochemical detection of cardiac troponin I in serum and saliva by nitrogen-doped porous reduced graphene oxide electrode, Sensor. Actuator. B Chem. 262 (2018) 180–187, https://doi.org/10.1016/j.snb.2018.01.215.